π and ρ mesons, and their diquark partners, from a contact interaction

H. L. L. Roberts,[1,2,3] A. Bashir,[4,5] L. X. Gutiérrez-Guerrero,[4] C. D. Roberts,[1,2,5,6] and D. J. Wilson[1]

[1]*Physics Division, Argonne National Laboratory, Argonne, Illinois 60439, USA*

[2]*Institut für Kernphysik, Forschungszentrum Jülich, D-52425 Jülich, Germany*

[3]*Physics Department, University of California, Berkeley, California 94720, USA*

[4]*Instituto de Física y Matemáticas, Universidad Michoacana de San Nicolás de Hidalgo, Morelia, Michoacán 58040, Mexico*

[5]*Kavli Institute for Theoretical Physics China, CAS, Beijing 100190, China*

[6]*Department of Physics, Center for High Energy Physics and the State Key Laboratory of Nuclear Physics and Technology, Peking University, Beijing 100871, China*

(Received 21 February 2011; published 22 June 2011)

We present a unified Dyson-Schwinger equation treatment of static and electromagnetic properties of pseudoscalar and vector mesons, and scalar and axial-vector diquark correlations, based upon a vector-vector contact interaction. A basic motivation for this paper is the need to document a comparison between the electromagnetic form factors of mesons and those diquarks that play a material role in nucleon structure. A notable result, therefore, is the large degree of similarity between related meson and diquark form factors. The simplicity of the interaction enables computation of the form factors at arbitrarily large spacelike Q^2, which enables us to expose a zero in the ρ-meson electric form factor at $z_Q^\rho \approx \sqrt{6} m_\rho$. Notably, $r_\rho z_Q^\rho \approx r_D z_Q^D$, where r_ρ and r_D are, respectively, the electric radii of the ρ-meson and deuteron.

DOI: 10.1103/PhysRevC.83.065206 PACS number(s): 13.20.−v, 13.40.Gp, 11.15.Tk, 24.85.+p

I. INTRODUCTION

In numerous respects, π and ρ mesons are the simplest bound states to study in QCD. That is, of course, supposing that the framework employed is Poincaré-covariant, capable of simultaneously implementing light-quark confinement and expressing dynamical chiral symmetry breaking (DCSB), and admits a global-symmetry-preserving truncation scheme. All these features are required because, amongst many other things, the pion is the lightest hadron and QCD's Goldstone mode, the ρ meson couples strongly to two pions and is an important part of the photon's vacuum polarization, and modern facilities probe hadrons with momentum transfers far in excess of any reasonable constituent-quark-like mass scale.

The Dyson-Schwinger equations (DSEs) [1,2] provide an approach to hadron physics that is distinguished by its ability to satisfy these demands;[1] in addition, there is a large body of research that addresses π- and ρ-meson properties. For example, the analysis of static properties is reported in Refs. [7–27] and of interactions in Refs. [28–47]. There is nevertheless a need to return to this theme, namely, a program aimed at charting the interaction between light quarks by explicating the impact of differing assumptions about the behavior of the Bethe-Salpeter kernel on hadron elastic and transition form factors [48].

To expose the connection, we remark that, in quantum field theory, a baryon appears as a pole in a six-point quark Green's function. The pole's residue is proportional to the baryon's Faddeev amplitude, which is obtained from a Poincaré-covariant Faddeev equation that sums all possible quantum-field-theoretical exchanges and interactions that can take place between three dressed quarks. A tractable truncation of the Faddeev equation is based [49] on the observation that an interaction which describes mesons also generates diquark correlations in the color-$\bar{3}$ channel [9]. The dominant correlations for ground-state octet and decuplet baryons are scalar (0^+) and axial-vector (1^+) diquarks because, for example, the associated mass scales are smaller than the baryons' masses and their parity matches that of these baryons. This is elucidated in Ref. [50].

At leading order in a global-symmetry-preserving truncation of the DSEs [15,17], simple changes in the equations describing π and ρ mesons yield expressions that provide detailed information about the scalar and axial-vector diquarks, e.g., their masses [9,10,18,23,50,51], and electromagnetic elastic [41] and transition form factors, which are critical elements in the computation of a baryon's kindred properties. It is therefore natural to elucidate concurrently the properties of π and ρ mesons and those of the scalar and axial-vector diquark correlations because it opens the way to a unified, symmetry-preserving explanation of meson and baryon properties as they are predicted by a single interaction. The potential of this approach is apparent in Refs. [52,53], but it has yet to be fully realized. For the present, the best connection is provided by the less rigorous approach of Ref. [54], which uses more parameters to express features of QCD, but also predicts and describes simultaneously a larger array of phenomena [55–57].

Herein, as part of the program outlined above, we describe results for a range of static and dynamic properties of these simplest u/d mesons and diquark correlations as produced by a vector-vector current-current interaction that is mediated by a momentum-independent boson propagator, i.e., by the symmetry-preserving regularization of a contact interaction. Given the large body of work based on QCD-like vector-boson

[1]Within the DSE framework, gauge invariance follows from gauge covariance, with which a truncation is imbued via the dressed-quark-gluon vertex. A prescription and program exist for addressing this challenge (see, e.g., Refs. [3–6]).

propagation that is already available, this paper will provide numerous points for comparison and contrast that are relevant to existing and planned experiments.

In Sec. II, we describe a global-symmetry-preserving regularization and DSE formulation of the contact interaction, following Refs. [44,46,50]. Our scheme is such that confinement is manifest, and chiral symmetry and the pattern by which it is broken are veraciously represented. In addition to the current-quark mass, the model has two parameters. In Sec. III, we describe results for π- and ρ-meson electromagnetic elastic and transition form factors, computed using the rainbow-ladder truncation of the DSEs, with the analogous discussion of diquark correlations reported in Sec. IV. Section V provides a summary and perspective.

II. CONTACT VECTOR-CURRENT-CURRENT INTERACTION

A. Gap equation

The typical starting point for a DSE study of hadron phenomena is the dressed-quark propagator, which is obtained from the gap equation

$$S(p)^{-1} = i\gamma\cdot p + m + \int \frac{d^4q}{(2\pi)^4} g^2 D_{\mu\nu}(p-q)\frac{\lambda^a}{2}\gamma_\mu S(q)\frac{\lambda^a}{2}\Gamma_\nu(q,p), \tag{1}$$

where m is the Lagrangian current-quark mass, $D_{\mu\nu}$ is the vector-boson propagator, and Γ_ν is the quark–vector-boson vertex. Much is now known about $D_{\mu\nu}$ in QCD [58–61], and nonperturbative information is accumulating on Γ_ν [4,6,26,62,63].

However, our goal is to build a stock of material that can be used to identify unambiguous signals in experiment for the pointwise behavior of the interaction between light quarks, the light quarks' mass function, and other similar quantities. While these are particular qualities, taken together they will enable a characterization of the nonperturbative behavior of the theory underlying strong interaction phenomena [45,48]. We therefore elucidate predictions following from the assumption

$$g^2 D_{\mu\nu}(p-q) = \delta_{\mu\nu}\frac{1}{m_G^2}, \tag{2}$$

where m_G is a gluon mass scale, and proceed by embedding this interaction in a rainbow-ladder truncation of the DSEs, which is the leading order in the most widely used, global-symmetry-preserving truncation scheme [17]. This means

$$\Gamma_\nu(p,q) = \gamma_\nu \tag{3}$$

in Eq. (1) and in the subsequent construction of the Bethe-Salpeter kernels.

One may view the interaction in Eq. (2) as being inspired by models of the Nambu-Jona-Lasinio type [64]. However, as will become clear, our treatment is atypical. It is also worth remarking that Eq. (2) is an antithetical complement to the interaction proposed in Ref. [65], i.e., a δ function in four-momentum space, which is confining because it provides a strong interaction that is independent of separation, x^2.

Using Eqs. (2) and (3), the gap equation becomes

$$S^{-1}(p) = i\gamma\cdot p + m + \frac{4}{3}\frac{1}{m_G^2}\int\frac{d^4q}{(2\pi)^4}\gamma_\mu S(q)\gamma_\mu, \tag{4}$$

an equation in which the integral possesses a quadratic divergence, even in the chiral limit. If the divergence is regularized in a Poincaré-covariant manner, then the solution is

$$S(p)^{-1} = i\gamma\cdot p + M, \tag{5}$$

where M is momentum independent and determined by

$$M = m + \frac{M}{3\pi^2 m_G^2}\int_0^\infty ds\, s\,\frac{1}{s+M^2}. \tag{6}$$

One must specify a regularization procedure in order to proceed. We write [66]

$$\frac{1}{s+M^2} = \int_0^\infty d\tau\, e^{-\tau(s+M^2)} \to \int_{\tau_{\rm uv}^2}^{\tau_{\rm ir}^2} d\tau\, e^{-\tau(s+M^2)} \tag{7}$$

$$= \frac{e^{-(s+M^2)\tau_{\rm uv}^2} - e^{-(s+M^2)\tau_{\rm ir}^2}}{s+M^2}, \tag{8}$$

where $\tau_{\rm ir,uv}$ are, respectively, infrared and ultraviolet regulators. It is apparent from Eq. (8) that a finite value of $\tau_{\rm ir} =: 1/\Lambda_{\rm ir}$ implements confinement by ensuring the absence of quark production thresholds [67,68]. We note that, since Eq. (2) does not define a renormalizable theory, $\Lambda_{\rm uv} := 1/\tau_{\rm uv}$ cannot be removed but instead plays a dynamical role and sets the scale of all dimensioned quantities. The gap equation can now be written as

$$M = m + \frac{M}{3\pi^2 m_G^2}\mathcal{C}^{\rm iu}(M^2), \tag{9}$$

where $\mathcal{C}^{\rm iu}(M^2)/M^2 = \Gamma(-1, M^2\tau_{\rm uv}^2) - \Gamma(-1, M^2\tau_{\rm ir}^2)$, with $\Gamma(\alpha, y)$ being the incomplete gamma function.

B. Point-meson Bethe-Salpeter equation

In rainbow-ladder truncation, with the interaction in Eq. (2), the homogeneous Bethe-Salpeter equation for a color-singlet meson is

$$\Gamma(k;P) = -\frac{4}{3}\frac{1}{m_G^2}\int\frac{d^4q}{(2\pi)^4}\gamma_\mu\chi(q;P)\gamma_\mu, \tag{10}$$

where $\chi(q;P) = S(q+P)\Gamma(q;P)S(q)$ and $\Gamma(q;P)$ is the meson's Bethe-Salpeter amplitude. Since the integrand does not depend on the external relative momentum k, then a symmetry-preserving regularization of Eq. (10) will yield solutions that are independent of k. It follows that, if the interaction in Eq. (2) produces bound states, then the relative momentum between the bound state's constituents can assume any value with equal probability. This is the defining characteristic of a pointlike composite particle.

With a dependence on the relative momentum forbidden by the interaction, the pseudoscalar and vector Bethe-Salpeter amplitudes take the general form[2] [69]

$$\Gamma^{\pi}(P) = i\gamma_5 E_{\pi}(P) + \frac{1}{M}\gamma_5 \gamma\cdot P F_{\pi}(P), \tag{11}$$

$$\Gamma^{\rho}_{\mu}(P) = \gamma^T_{\mu} E_{\rho}(P) + \frac{1}{M}\sigma_{\mu\nu} P_{\nu} F_{\rho}(P), \tag{12}$$

where $P_\mu \gamma^T_\mu = 0$ and $\gamma^T_\mu + \gamma^L_\mu = \gamma_\mu$. We observe that

$$F_{\rho}(P) \overset{\text{ladder}}{\equiv} 0\,. \tag{13}$$

However, it should be kept in mind that this is an artifact of the rainbow-ladder truncation; viz., even using Eq. (2), $F_\rho(P) \neq 0$ in any symmetry-preserving truncation that goes beyond this leading order [17]. We will see that the accident expressed in Eq. (13) has material consequences.

C. Ward-Takahashi identities

No study of π- or ρ-meson observables is meaningful unless it ensures expressly that the vector and axial-vector Ward-Takahashi identities are satisfied. The $m = 0$ axial-vector identity states ($k_+ = k + P$)

$$P_\mu \Gamma_{5\mu}(k_+, k) = S^{-1}(k_+) i\gamma_5 + i\gamma_5 S^{-1}(k), \tag{14}$$

where $\Gamma_{5\mu}(k_+, k)$ is the axial-vector vertex, which is determined by

$$\Gamma_{5\mu}(k_+, k) = \gamma_5\gamma_\mu - \frac{4}{3}\frac{1}{m_G^2}\int \frac{d^4q}{(2\pi)^4}\,\gamma_\alpha \chi_{5\mu}(q_+, q)\gamma_\alpha\,. \tag{15}$$

We must therefore implement a regularization that maintains Eq. (14). This requirement is readily found to entail the following two chiral limit identities [44]:

$$M = \frac{8}{3}\frac{M}{m_G^2}\int \frac{d^4q}{(2\pi)^4}\left[\frac{1}{q^2 + M^2} + \frac{1}{q_+^2 + M^2}\right], \tag{16}$$

$$0 = \int \frac{d^4q}{(2\pi)^4}\left[\frac{P\cdot q_+}{q_+^2 + M^2} - \frac{P\cdot q}{q^2 + M^2}\right], \tag{17}$$

which must be satisfied after regularization. By analyzing the integrands using a Feynman parametrization, one arrives at the following identities for $P^2 = 0 = m$:

$$M = \frac{16}{3}\frac{M}{m_G^2}\int \frac{d^4q}{(2\pi)^4}\frac{1}{[q^2 + M^2]}, \tag{18}$$

$$0 = \int \frac{d^4q}{(2\pi)^4}\frac{\frac{1}{2}q^2 + M^2}{[q^2 + M^2]^2}. \tag{19}$$

Equation (18) is just the chiral-limit gap equation. Hence, it requires nothing new of the regularization scheme. On the other hand, Eq. (19) states that the axial-vector Ward-Takahashi identity is satisfied if, and only if, the model is regularized so as to ensure that there are no quadratic or logarithmic divergences. Unsurprisingly, these are the just the circumstances under which a shift in integration variables is permitted, an operation required in order to prove Eq. (14).

It is notable, too, that Eq. (14) is valid for arbitrary P. In fact, its corollary [Eq. (16)] may be used to demonstrate that, in the chiral limit, the two-flavor scalar-meson rainbow-ladder truncation of the contact-interaction DSEs produces a bound state with mass $m_\sigma = 2M$ [50,70]. In the presence of a momentum-dependent dressed-quark mass function, one could reverse this association and define a chiral-limit dressed-quark constituent mass as one-half the mass of the lightest rainbow-ladder scalar meson. This procedure yields $M^0 \simeq 0.3$ GeV, as may readily be determined from Ref. [2].

The second corollary, Eq. (17), entails

$$0 = \int_0^1 d\alpha\,\left\{\mathcal{C}^{\rm iu}(\omega(M^2, \alpha, P^2)) + \mathcal{C}_1^{\rm iu}(\omega(M^2, \alpha, P^2))\right\}, \tag{20}$$

with

$$\omega(M^2, \alpha, P^2) = M^2 + \alpha(1-\alpha)P^2, \tag{21}$$

$$\begin{aligned}\mathcal{C}_1^{\rm iu}(z) &= -z(d/dz)\mathcal{C}^{\rm iu}(z)\\ &= z\left[\Gamma\left(0, M^2 r_{\rm uv}^2\right) - \Gamma\left(0, M^2 r_{\rm ir}^2\right)\right].\end{aligned} \tag{22}$$

The vector Ward-Takahashi identity

$$P_\mu i\Gamma^\gamma_\mu(k_+, k) = S^{-1}(k_+) - S^{-1}(k), \tag{23}$$

where Γ^γ_μ is the dressed-quark–photon vertex, is crucial for a sensible study of electromagnetic form factors [29]. Ideally, the vertex needs to be dressed at a level consistent with the truncation used to compute the bound state's Bethe-Salpeter amplitude [33]. In our case, this means the vertex should be determined from the following inhomogeneous Bethe-Salpeter equation:

$$\Gamma_\mu(Q) = \gamma_\mu - \frac{4}{3}\frac{1}{m_G^2}\int \frac{d^4q}{(2\pi)^4}\,\gamma_\alpha \chi_\mu(q_+, q)\gamma_\alpha, \tag{24}$$

where $\chi_\mu(q_+, q) = S(q+P)\Gamma_\mu(Q)S(q)$. Owing to the momentum-independent nature of the interaction kernel, the general form of the solution is

$$\Gamma_\mu(Q) = \gamma^T_\mu P_T(Q^2) + \gamma^L_\mu P_L(Q^2), \tag{25}$$

where $Q_\mu \gamma^T_\mu = 0$ and $\gamma^T_\mu + \gamma^L_\mu = \gamma_\mu$. This simplicity does not survive with a more sophisticated interaction nor with Eq. (2) beyond rainbow-ladder truncation [50].

By inserting Eq. (25) into Eq. (24), one readily obtains

$$P_L(Q^2) = 1, \tag{26}$$

owing to Eq. (17). By using this same identity, one finds

$$P_T(Q^2) = \frac{1}{1 + K_\gamma(Q^2)}, \tag{27}$$

with [$\overline{\mathcal{C}}_1(z) = \mathcal{C}_1(z)/z$]

$$K_\gamma(Q^2) = \frac{1}{3\pi^2 m_G^2} \times \int_0^1 d\alpha\,\alpha(1-\alpha)Q^2\,\overline{\mathcal{C}}_1^{\rm iu}[\omega(M^2, \alpha, Q^2)]\,. \tag{28}$$

Plainly,

$$P_T(Q^2 = 0) = 1, \tag{29}$$

[2] We assume isospin symmetry throughout and hence do not include the Pauli isospin matrices explicitly.

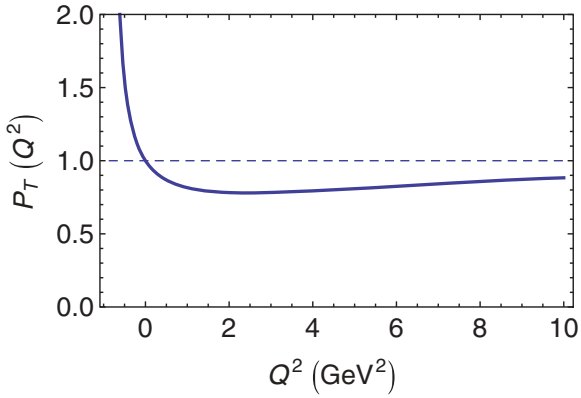

FIG. 1. (Color online) Dressing function for the transverse piece of the quark-photon vertex; viz., $P_T(Q^2)$ in Eq. (27), computed using the parameter values described in connection with Table I.

so that at $Q^2 = 0$ in the rainbow-ladder treatment of the interaction in Eq. (2), the dressed-quark-photon vertex is equal to the bare vertex.[3]

However, this is not true for $Q^2 \neq 0$. In fact, the transverse part of the dressed-quark-photon vertex will display a pole at $Q^2 < 0$ for which

$$1 + K_\gamma(Q^2) = 0\,. \tag{30}$$

This is just the model's Bethe-Salpeter equation for the ground-state vector meson.

In Fig. 1, we depict the function that dresses the transverse part of the quark-photon vertex. The pole associated with the ground-state vector meson is clear. This is accompanied by a minimum at spacelike Q^2, a feature observed in all computations of the dressed-quark-gluon vertex (see, e.g., Ref. [33]). The minimum arises because, in an internally consistent computation, spectral strength in the 1^{--} channel is shifted to the ρ-meson pole. One cannot simultaneously satisfy the Ward-Takahashi identity $P_T(Q^2 = 0) = 1$ and exhibit the ρ pole unless the dressing function is depleted for $Q^2 > 0$. The precise location and depth of the minimum are model dependent, but its existence is model independent. Another important feature is the behavior at large spacelike Q^2, namely, $P_T(Q^2) \to 1^-$ as $Q^2 \to \infty$. This is the statement that a dressed quark is pointlike to a large-Q^2 probe. The same is true in QCD up to the logarithmic corrections, which are characteristic of an asymptotically free theory [33].

D. Bethe-Salpeter kernels for π and ρ

At this point, we can write the explicit form of Eq. (10) for the pion as

$$\begin{bmatrix} E_\pi(P) \\ F_\pi(P) \end{bmatrix} = \frac{1}{3\pi^2 m_G^2} \begin{bmatrix} \mathcal{K}_{EE} & \mathcal{K}_{EF} \\ \mathcal{K}_{FE} & \mathcal{K}_{FF} \end{bmatrix} \begin{bmatrix} E_\pi(P) \\ F_\pi(P) \end{bmatrix}, \tag{31}$$

where

$$\mathcal{K}_{EE} = \int_0^1 d\alpha \big\{ \mathcal{C}^{\rm iu}\big(\omega\big(M^2, \alpha, -m_\pi^2\big)\big) + 2\alpha(1-\alpha)\, m_\pi^2\, \bar{\mathcal{C}}_1^{\rm iu}\big(\omega\big(M^2, \alpha, -m_\pi^2\big)\big)\big\}, \tag{32}$$

$$\mathcal{K}_{EF} = -m_\pi^2 \int_0^1 d\alpha\, \bar{\mathcal{C}}_1^{\rm iu}\big(\omega\big(M^2, \alpha, -m_\pi^2\big)\big), \tag{33}$$

$$\mathcal{K}_{FE} = \frac{1}{2} M^2 \int_0^1 d\alpha\, \bar{\mathcal{C}}_1^{\rm iu}\big(\omega\big(M^2, \alpha, -m_\pi^2\big)\big), \tag{34}$$

$$\mathcal{K}_{FF} = -2\mathcal{K}_{FE}. \tag{35}$$

This is an eigenvalue problem for the pion mass-squared m_π^2. Note that we used Eq. (20) to arrive at Eq. (35).

The explicit form of Eq. (10) for the ρ meson, the solution of which yields its mass-squared, is

$$1 + K_\gamma\big(-m_\rho^2\big) = 0, \tag{36}$$

where K_γ is given in Eq. (28).

In the computation of observables, one must use the canonically normalized Bethe-Salpeter amplitudes. For the rainbow-ladder pion, this means that Γ_π is rescaled to satisfy

$$P_\mu = N_c\, \mathrm{tr} \int \frac{d^4q}{(2\pi)^4} \Gamma_\pi(-P) \frac{\partial}{\partial P_\mu} S(q+P)\, \Gamma_\pi(P)\, S(q), \tag{37}$$

which, in the chiral limit, becomes

$$1 = \frac{N_c}{4\pi^2} \frac{1}{M^2}\, \mathcal{C}_1\big(M^2; \tau_{\rm ir}^2, \tau_{\rm uv}^2\big) E_\pi [E_\pi - 2F_\pi]. \tag{38}$$

For the rainbow-ladder ρ meson, on the other hand, the vector meson analog of Eq. (37) requires that

$$\frac{1}{E_\rho^2} = -9 m_G^2 \frac{d}{dz} K_\gamma(z)\Big|_{z=-m_\rho^2}. \tag{39}$$

In terms of the canonically normalized Bethe-Salpeter amplitudes, the leptonic decay constants of the π and ρ mesons are, respectively, given by

$$f_\pi = \frac{1}{M} \frac{3}{2\pi^2} [E_\pi - 2F_\pi]\, \mathcal{K}_{FE}^{P^2=-m_\pi^2}, \tag{40}$$

$$f_\rho = -\frac{9}{2} \frac{E_\rho}{m_\rho} K_\gamma\big(-m_\rho^2\big)\,. \tag{41}$$

Another important low-energy property is the in-pion condensate[4]

$$\kappa_\pi = f_\pi \frac{3}{4\pi^2} \big[E_\pi \mathcal{K}_{EE}^{P^2=-m_\pi^2} + F_\pi\, \mathcal{K}_{EF}^{P^2=-m_\pi^2}\big]. \tag{42}$$

In the chiral limit, $\kappa_\pi \to \kappa_\pi^0 = -\langle \bar{q} q \rangle$, i.e., the so-called vacuum quark condensate [72]. Moreover, in this limit, too, one can readily verify that [44]

$$E_\pi \overset{m=0}{=} \frac{M}{f_\pi}, \tag{43}$$

[3]Equations (26) and (29) guarantee a massless photon and show that our regularization also ensures preservation of the Ward-Takahashi identity for the photon vacuum polarization [71].

[4]There is an analogous in-ρ-meson condensate but that will be discussed elsewhere.

TABLE I. Results obtained with (in GeV) $m_G = 0.132$, $\Lambda_{\rm ir} = 0.24$, and $\Lambda_{\rm uv} = 0.905$, which yield a root-mean-square relative error of 13% in comparison with our specified goals for the observables. Dimensioned quantities are listed in GeV.

m	E_π	F_π	E_ρ	M	$\kappa_\pi^{1/3}$	m_π	m_ρ	f_π	f_ρ
0	3.568	0.459	1.520	0.358	0.241	0	0.919	0.100	0.130
0.007	3.639	0.481	1.531	0.368	0.243	0.140	0.928	0.101	0.129

which is a particular case of one of the Goldberger-Treiman relations proved in Ref. [19], and $F_\pi(P=0)$ satisfies a similar identity.

III. π AND ρ ELASTIC AND TRANSITION FORM FACTORS

In order to compute the form factors, we need to fix the model's two parameters, namely, m_G and $\Lambda_{\rm uv}$.[5] We do that by performing a least-squares fit in the chiral limit to [44,46, 73–75] $M^0 = 0.40\,$GeV, $\kappa_\pi^0 = (0.22\ \text{GeV})^3$, $f_\pi^0 = 0.088$ GeV, $m_\rho^0 = 0.78$ GeV, and $f_\rho^0 = 0.15$ GeV. This procedure yields the results in Table I. We remark that, in fitting, the same weight was given to each quantity because they are equally important. In dealing with electromagnetic form factors, some might suppose that one should lean more heavily toward obtaining the empirical value of m_ρ. However, the dressed-quark mass, in-pion condensate, and pion-leptonic decay constant are low-energy observables that are just as important as m_ρ. Furthermore, attempts to suppress the value of m_ρ lead invariably to a marked reduction in the value of f_ρ, e.g., a 20% reduction in m_G and a 10% reduction in $\Lambda_{\rm uv}$, produce $m_\rho = 0.91$ GeV (a 2% reduction) and $f_\rho = 0.11$ GeV (a 15% reduction). Given the importance of f_ρ in electromagnetic processes, it must be weighted at least equally with m_ρ. A description of static pion and ρ-meson observables with a 13% root-mean-square relative error, in which m_ρ is just 19% too large and f_ρ is 13% too small, is the best result achievable in an internally consistent, symmetry-preserving treatment of the vector-vector contact interaction we have defined.

It is worth observing that m_G is merely the single parameter that we have chosen to characterize $g^2 D_{\mu\nu}(p-q)$ in Eq. (2). We could equally have written $g^2 D = 4\pi\alpha_{\rm ir}/[m_G^{\rm ol}]^2$, where $m_G^{\rm ol} = 0.8$ GeV is a mass scale typical of the one-loop renormalization-group-improved interaction introduced in Refs. [20,22]. With this alternative prescription, $m_G = 0.132$ GeV corresponds to $\alpha_{\rm ir}/\pi = 0.93$, a magnitude commensurate with contemporary estimates of the zero-momentum value of a running coupling in QCD [75–78].

A. π-meson elastic form factors

We are solving the interaction of Eq. (2) in the rainbow-ladder truncation, i.e., at leading order in the nonperturbative global-symmetry-preserving truncation of Refs. [15,17]. At this order, the generalized impulse approximation is computed for three-point scattering processes [29], such as elastic form factors. An analysis of the associated triangle diagram yields the formulae in the Appendix and the computed result is depicted in Fig. 2. Two features are immediately apparent, viz., the pole associated with the ρ meson at timelike momentum, which is a consequence of dressing the quark-photon vertex, and a momentum-independent interaction produces $F_\pi(Q^2) =$ constant as $Q^2 \to \infty$. The following function is a valid interpolation of the full result on the domain shown:

$$F_\pi^{\rm em}(Q^2) \stackrel{\text{interpolation}}{=} \frac{1 + 0.33\,Q^2 + 0.024\,Q^4}{1 + 1.20\,Q^2 + 0.053\,Q^4}. \tag{44}$$

In Table II, we report the pion charge radius

$$r_\pi^2 = -6\frac{d}{dQ^2}F_\pi(Q^2)\Big|_{Q^2=0}. \tag{45}$$

The result is less than experiment ($r_\pi = 0.672 \pm 0.008$ fm [79]). This is due in small part to our omission of pseudoscalar meson rescattering effects [80] but more to the large value we obtain for the ρ meson's mass. It cannot be remedied in our global-symmetry-preserving rainbow-ladder treatment of Eq. (2) because all dimensioned quantities are too closely tied to the value of M. An interaction that preserves the one-loop renormalization-group behavior of QCD [20,22] provides decoupling between the values of ultraviolet and infrared phenomena, such as κ_π and m_ρ.

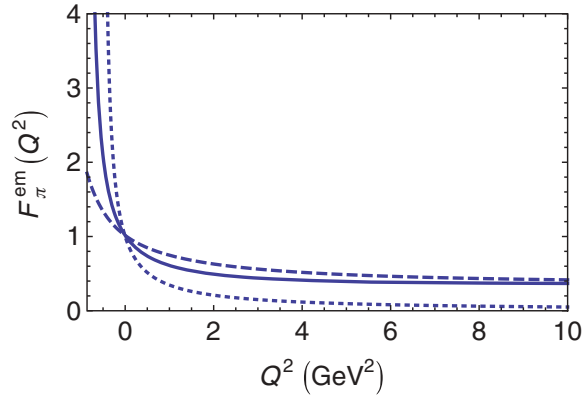

FIG. 2. (Color online) $F_\pi^{\rm em}(Q^2)$ computed in rainbow-ladder truncation from the interaction in Eq. (2). Solid curve: Fully consistent, i.e., with a dressed-quark-photon vertex so that the ρ pole appears. Dashed curve: Computed using a bare quark-photon vertex. Dotted curve: Fit to the result in Ref. [35], which was obtained with a momentum-dependent interaction that preserves the one-loop renormalization-group behavior of QCD, included a consistently dressed-quark-photon vertex, and serves to illustrate the trend of contemporary data.

[5] We fix $\Lambda_{\rm ir} = 0.24$ GeV $\approx \Lambda_{\rm QCD}$ since $r_{\rm QCD} := 1/\Lambda_{\rm QCD} \approx 0.8$ fm is a length scale typical of confinement.

TABLE II. Row 1: Form factor radii (in fm), and magnetic and quadrupole moments for the ρ meson $G_M^\rho(Q^2=0)$ and $G_Q^\rho(Q^2=0)$, respectively, computed with (in GeV) $m=0.007$, $m_G=0.132$, $\Lambda_{\rm ir}=0.24$, and $\Lambda_{\rm uv}=0.905$. For a structureless vector meson, $\mu=2$ and $\mathcal{Q}=-1$ [81]. The next four rows list results reported elsewhere. Experimentally, $r_\pi=0.672\pm0.008$ fm [79]. (Note that none of the quoted computations included contributions from nonresonant pseudoscalar-meson final-state interactions and, hence, agreement with the experimental value of r_π should be seen as a defect of the associated model [80]. The nature of this flaw is understood within the DSE context, where such contributions can be viewed as computable corrections to the rainbow-ladder truncation [52].) The last two lines report results for the scalar and axial-vector diquark correlations. Here, the magnetic and quadrupole moments should be multiplied by the relevant charge factor, viz., $e_{\{uu\}}=\frac{4}{3}$, $e_{\{ud\}}=\frac{1}{3}$, and $e_{\{dd\}}=-\frac{2}{3}$.

	r_π	r_ρ^E	r_ρ^M	r_ρ^E	μ_ρ	$\mathcal{Q}_\rho$
This work	0.45	0.56	0.51	0.51	2.11	−0.85
Ref. [43]	0.66	0.73			2.01	−0.41
Refs. [82,83]	0.56	0.61			2.69	−0.84
Refs. [84,85]	0.66	0.61			2.14	−0.79
Refs. [86,87]	0.66	0.52			1.92	−0.43
	r_{0^+}	$r_{1^+}^E$	$r_{1^+}^M$	$r_{1^+}^E$	μ_{1^+}	$\mathcal{Q}_{1^+}$
This work	0.49	0.55	0.51	0.51	2.13	−0.81
Ref. [41]	0.71					

B. ρ-meson elastic form factors

The $J^{PC}=1^{--}$ ρ meson has three elastic form factors and we follow Ref. [43] in defining them. By denoting the incoming photon momentum by Q, and the incoming and outgoing ρ-meson momenta by $p^i=K-Q/2$ and $p^f=K+Q/2$, then $K\cdot Q=0$, $K^2+Q^2/4=-m_\rho^2$, and the ρ-γ-ρ vertex can be expressed as

$$\Lambda_{\lambda,\mu\nu}(K,Q)=\sum_{j=1}^{3}T^j_{\lambda,\mu\nu}(K,Q)\,F_j(Q^2), \tag{46}$$

$$T^1_{\lambda,\mu\nu}(K,Q)=2K_\lambda\,\mathcal{P}^T_{\mu\alpha}(p^i)\,\mathcal{P}^T_{\alpha\nu}(p^f), \tag{47}$$

$$T^2_{\lambda,\mu\nu}(K,Q)=\left[Q_\mu-p^i_\mu\frac{Q^2}{2m_\rho^2}\right]\mathcal{P}^T_{\lambda\nu}(p^f) -\left[Q_\nu+p^f_\nu\frac{Q^2}{2m_\rho^2}\right]\mathcal{P}^T_{\lambda\mu}(p^i), \tag{48}$$

$$T^3_{\lambda,\mu\nu}(K,Q)=\frac{K_\lambda}{m_\rho^2}\left[Q_\mu-p^i_\mu\frac{Q^2}{2m_\rho^2}\right]\left[Q_\nu+p^f_\nu\frac{Q^2}{2m_\rho^2}\right], \tag{49}$$

where $\mathcal{P}^T_{\mu\nu}(p)=\delta_{\mu\nu}-p_\mu p_\nu/p^2$. A symmetry-preserving regularization scheme is essential here so that the following identities are preserved throughout the analysis:

$$Q_\lambda\Lambda_{\lambda,\mu\nu}(K,Q)=0, \tag{50}$$

$$p^i_\mu\Lambda_{\lambda,\mu\nu}(K,Q)=0=p^f_\nu\Lambda_{\lambda,\mu\nu}(K,Q). \tag{51}$$

The electric, magnetic, and quadrupole form factors are constructed as follows:

$$G_E^\rho(Q^2)=F_1(Q^2)+\tfrac{2}{3}\eta G_Q(Q^2), \tag{52}$$

$$G_M^\rho(Q^2)=-F_2(Q^2), \tag{53}$$

$$G_Q^\rho(Q^2)=F_1(Q^2)+F_2(Q^2)+[1+\eta]F_3(Q^2), \tag{54}$$

where $\eta=Q^2/[4m_\rho^2]$. In the limit $Q^2\to0$, these form factors define the charge, and magnetic and quadrupole moments of the ρ meson, viz.,

$$G_E^\rho(Q^2=0)=1, \tag{55}$$

$$G_M^\rho(Q^2=0)=\mu_\rho,\quad G_Q^\rho(Q^2=0)=\mathcal{Q}_\rho. \tag{56}$$

It is readily seen that Eq. (55) is a symmetry constraint. One has $G_E(Q^2=0)=F_1(Q^2=0)$ and

$$\Lambda_{\lambda,\mu\nu}(K,Q)\stackrel{Q^2\to0}{=}2K_\lambda\,\mathcal{P}^T_{\mu\alpha}(K)\,\mathcal{P}^T_{\alpha\nu}(K)\,F_1(0). \tag{57}$$

By using Eqs. (23), (27), and (A10), this becomes

$$K_\lambda\,\mathcal{P}^T_{\mu\nu}(K)F_1(0) =N_c E_\rho^2{\rm tr}_D\int\frac{d^4q}{(2\pi^4)}i\gamma_\nu\frac{\partial}{\partial K_\lambda}S(\ell+K)i\gamma_\mu\,S(\ell). \tag{58}$$

The right-hand-side is simply the analog of Eq. (37) for the rainbow-ladder vector meson. Hence, when E_ρ is normalized according to Eq. (39) and so long as one employs a global-symmetry-preserving regularization procedure, the right-hand side is equal to $K_\lambda\,\mathcal{P}^T_{\mu\nu}(K)$ and thus $F_1(0)=1$.

We compute the form factors using the formulae in the Appendix. In Table II, we report form-factor radii and the magnetic and quadrupole moments. The comments following Eq. (45) are also relevant to the magnitudes of the ρ-meson radii.

From the table, we find $r_\pi/r_\rho=0.80$. However, an interpretation of this value is not straightforward because we have consistently used the rainbow-ladder truncation, and whereas $F_\pi(P)\neq0$ always, $F_\rho(P)=0$ in rainbow-ladder truncation. [Note that in all more sophisticated truncations, $F_\rho(P)\neq0$.] Another relevant comparison may therefore be obtained if one artificially sets $F_\pi(P)=0$ when computing the pion form factor. This yields $r_\pi=0.51$ fm and, therefore, $r_\pi/r_\rho=0.92$. Now, the DSE computation in Ref. [43], which employs a QCD-based interaction, produces $r_\pi/r_\rho=0.90$, and, in combination, the more phenomenological DSE studies of Refs. [82,83] yield $r_\pi/r_\rho=0.92$. This context establishes that our result is actually typical of studies in which the structure of π and ρ mesons is treated equally.

Our computed ρ-meson electric form factor is plotted in Fig. 3. It displays a zero at $Q^2=5.0$ GeV^2 and remains negative thereafter. Given that the deuteron is a weakly bound $J=1$ system, constituted from two fermions, and its electric form factor possesses a zero [88], it is unsurprising that $G_E^\rho(Q^2)$ exhibits a zero. It is notable, in addition, that the deuteron's zero is located at $z_Q^D:=\sqrt{Q^2}=0.8$ GeV, so that

$$z_Q^D r_D\approx z_Q^\rho r_\rho^E, \tag{59}$$

where r_D is the deuteron's radius. An interpolation valid on $Q^2\in[-m_\rho^2,10\ {\rm GeV}^2]$ is

$$G_E^\rho(Q^2)\stackrel{\rm interpolation}{=}\frac{1-0.20\,Q^2}{1+1.15\,Q^2-0.013\,Q^4}. \tag{60}$$

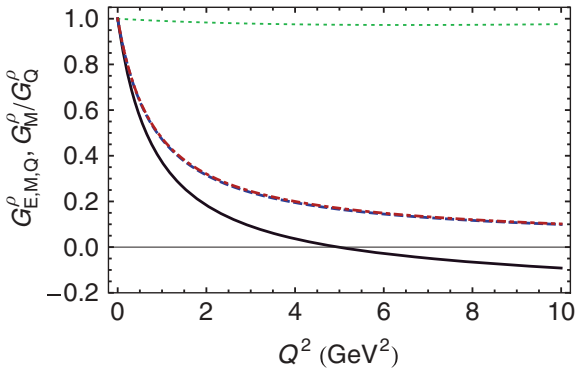

FIG. 3. (Color online) Solid curve: ρ-meson electric form factor $G^\rho_E(Q^2)$, which exhibits a zero at $Q^2 = 5.0$ GeV^2. (It is notable that $1 - \frac{2}{3}\eta = 0$ for $Q^2 = 6m_\rho^2 = 5.2$ GeV^2.) The dashed curve $G^\rho_M(Q^2)/\mu_\rho$ and dotted-dashed curve $G^\rho_Q(Q^2)/\mathcal{Q}_\rho$ are almost indistinguishable, as emphasised by the dotted curve $[G^\rho_M(Q^2)/\mu_\rho]/[G^\rho_Q(Q^2)/\mathcal{Q}_\rho]$. The charge radii and magnetic and quadrupole moments are given in Table II. Note that all form factors exhibit a pole at $Q^2 = -m_\rho^2$ because the quark-photon vertex is dressed as described in Sec. II C.

In Fig. 3, we also depict the magnetic and quadrupole form factors of the ρ meson, both normalized by their values at $Q^2 = 0$. Notably, neither of these two form factors change sign: for $Q^2 > -m_\rho^2$, $G^\rho_M(Q^2)$ is positive definite and $G^\rho_Q(Q^2)$ is negative definite.[6] It is worth remarking that, on this entire domain, $G^\rho_{M,Q}(Q^2)$ exhibit a very similar Q^2 dependence, which is made especially apparent via the dotted curve in Fig. 3. Interpolations valid on $Q^2 \in [-m_\rho^2, 10\,\text{GeV}^2]$ are

$$G^\rho_M(Q^2) \stackrel{\text{interpolation}}{=} \frac{2.11 + 0.021\,Q^2}{1 + 1.15\,Q^2 - 0.015\,Q^4}, \tag{61}$$

$$G^\rho_Q(Q^2) \stackrel{\text{interpolation}}{=} -\frac{0.85 + 0.038\,Q^2}{1 + 1.17\,Q^2 + 0.014\,Q^4}\,. \tag{62}$$

The similar momentum dependence of G^ρ_M and G^ρ_Q recalls a prediction in Ref. [81], namely,

$$G_E(Q^2) : G_M(Q^2) : G_Q(Q^2) \stackrel{Q^2\to\infty}{=} 1 - \tfrac{2}{3}\eta : 2 : -1 \tag{63}$$

in theories with a vector-vector interaction mediated via bosons propagating as $1/k^2$ at large k^2. Our computed ratio $r_{M/Q} := G^\rho_M(Q^2)/G^\rho_Q(Q^2)$ conforms approximately with this prediction on a large domain of Q^2, e.g.,

$$\begin{array}{cccccc} Q^2 & 0 & 10 & 10^2 & 10^3 \\ r_{M/Q} & -2.48 & -2.54 & -2.38 & -2.17 \end{array}\,. \tag{64}$$

However, at $Q^2 = 10^4$ GeV^2, $r_{M/Q} = -1.28$. Moreover, the remaining two ratios are always in conflict with the prediction; closer inspection reveals that even the apparent agreement for $G^\rho_M(Q^2)/G^\rho_Q(Q^2)$ is accidental, since Eq. (63) is true if, and only if,

$$F_1(Q^2) : F_2(Q^2) : Q^2 F_3(Q^2) \stackrel{Q^2\to\infty}{=} 1 : -2 : 0. \tag{65}$$

None of these predictions are satisfied in our computation.

The mismatch originates, of course, with Eq. (2) and the concomitant need for a regularization procedure in which the ultraviolet cutoff plays a dynamical role. If one carefully removes $\Lambda_{\text{uv}} \to \infty$, Eq. (65) is recovered but at the cost of a logarithmic divergence in the individual form factors. We therefore conclude that a vector-vector contact interaction cannot reasonably be regularized in a manner consistent with Eq. (63).

In closing this section, we reiterate that it is only in the rainbow-ladder truncation that $F_\rho(P) \equiv 0$. Therefore, in connection with the ρ meson's form factors, material changes should be anticipated when proceeding beyond this leading-order truncation.

C. ρ-π transition form factor

This transition is closely related to the $\gamma^*\pi\gamma$ transition form factor, whose behavior in connection with Eq. (2) was analyzed in Ref. [46]. The interaction vertex is expressed in Eq. (A18) and defines a single form factor, viz.,

$$T^{\pi\gamma\rho}_{\mu\nu}(k_1, k_2) = \frac{g_{\pi\gamma\rho}}{m_\rho}\,\epsilon_{\mu\nu\alpha\beta}k_{1\alpha}k_{2\beta}\,G^{\pi\gamma\rho}(Q^2), \tag{66}$$

where $k_1^2 = Q^2$, $k_2^2 = -m_\rho^2$. The coupling constant $g_{\pi\gamma\rho}$ is defined such that $G^{\pi\gamma\rho}(Q^2 = 0) = 1$, and explicit formulae for computing this form factor are provided in the Appendix.

Our computed form factor is depicted in Fig. 4. Naturally, because the quark-photon vertex is dressed (see Fig. 1), the transition form factor exhibits a pole at $Q^2 = -m_\rho^2$, which we have not displayed. An interpolation valid on $Q^2 \in [-m_\rho^2, 10\ \text{GeV}^2]$ is

$$G^{\pi\gamma\rho}(Q^2) \stackrel{\text{interpolation}}{=} \frac{1 + 0.37\,Q^2 + 0.024\,Q^4}{1 + 1.29\,Q^2 + 0.015\,Q^4}\,. \tag{67}$$

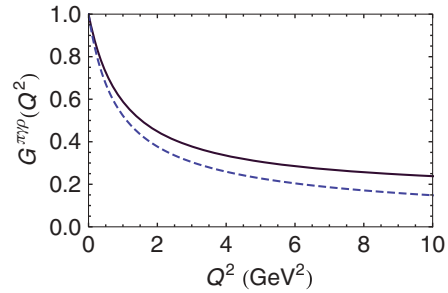

FIG. 4. (Color online) Solid curve: The full result for $G^{\pi\gamma\rho}(Q^2)$. Dashed curve: $G^{\pi\gamma\rho}(Q^2)$ obtained with $F_\pi(P) \equiv 0$. Experimentally [79], the partial width for $\rho^+ \to \pi^+\gamma$ is 68 ± 7 keV, which corresponds to a dimensionless coupling [38] $g_{\pi\gamma\rho} = (0.74 \pm 0.05)\,m_\rho/\text{GeV}$. This is in fair agreement with our computed result, viz., $g_{\pi\gamma\rho} = 0.63\,m_\rho/\text{Gev}$.

[6] In constituentlike quark models, $\mathcal{Q}_\rho = G^\rho_Q(Q^2 = 0) < 0$ corresponds to oblate deformation [89]. Contemporary lattice simulations arrive at a similar conclusion [90,91]. In this connection, it should be kept in mind that $\mathcal{Q} = G_Q(Q^2 = 0) = -1$ for a structureless $J = 1$ bound state [81].

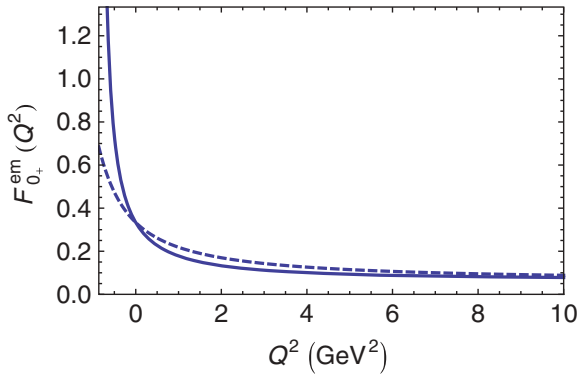

FIG. 5. (Color online) Solid curve: Full result for scalar-diquark elastic electromagnetic form factor. Dashed curve: Result obtained without dressing the quark-photon vertex. The computed mass of the diquark is $m_{qq_{0^+}} = 0.776$ GeV and the charge radius is given in Table II.

In the neighborhood of $Q^2 = 0$, the form factor is characterized by a radius-like length scale, viz.,

$$r^2_{\pi\gamma\rho} := -6\frac{d}{dQ^2}G^{\pi\gamma\rho}(Q^2)\Big|_{Q^2=0} = (0.46\ \text{fm})^2, \tag{68}$$

which is almost indistinguishable from both $r_\pi = 0.45$ fm in Table II and the anomaly interaction radius defined in Ref. [46], viz., $r^*_{\pi^0} = 0.48$ fm. On the other hand,

$$\lim_{Q^2\to\infty} G^{\pi\gamma\rho}(Q^2) = 0.11, \tag{69}$$

owing to the presence of the pion's pseudovector component, a result in keeping with the pointlike nature of bound states generated by a contact interaction [44,46].

IV. 0^+- AND 1^+-DIQUARK ELASTIC AND TRANSITION FORM FACTORS

A. Scalar-diquark elastic form factor

In the context of the interaction in Eq. (2), a detailed discussion of the relationship between pseudoscalar- and vector-mesons and scalar- and axial-vector-diquark correlations may be found in Ref. [50]. Using the information provided therein, it is straightforward to show that, in rainbow-ladder truncation, the electromagnetic form factor of a scalar diquark is readily obtained from the expression for $F^{\rm em}_\pi(Q^2)$. Namely,

$$F^{\rm em}_{0^+}(Q^2) = \tfrac{1}{3}F^{\rm em}_\pi(Q^2)\big|^{(E_\pi,F_\pi)\to\sqrt{\frac{2}{3}}(E_{qq_{0^+}},F_{qq_{0^+}})}_{m_\pi\to m_{qq_{0^+}}}, \tag{70}$$

where the scalar-diquark Bethe-Salpeter amplitude is expressed via ($C = \gamma_2\gamma_4$ is the charge-conjugation matrix)

$$\Gamma_{qq_{0^+}}(P)C^\dagger = \gamma_5\left[iE_{qq_{0^+}}(P) + \frac{1}{M}\gamma\cdot P F_{qq_{0^+}}(P)\right]. \tag{71}$$

Our result for the scalar-diquark elastic electromagnetic form factor is presented in Fig. 5. An interpolation valid on $Q^2 \in [-m^2_\rho, 10\ \text{GeV}^2]$ is

$$F^{\rm em}_{0^+}(Q^2) \overset{\text{interpolation}}{=} \frac{1}{3}\frac{1 + 0.25\,Q^2 + 0.027\,Q^4}{1 + 1.27Q^2 + 0.13\,Q^4}. \tag{72}$$

The normalization is different but the momentum dependence is similar to that of $F^{\rm em}_\pi$. This is indicated, too, by the ratio of charge radii, viz., $r_{0^+}/r_\pi = 1.08$, which may be compared to the value of 1.09 obtained in Ref. [41] and contrasted with the value of 0.8 in [92]. In the absence of the scalar-diquark Bethe-Salpeter amplitude's pseudovector component $F_{qq_{0^+}} \equiv 0$, we find $r_{0^+} = 0.51$ fm, i.e., an increase of 6%.

B. Pseudovector-diquark elastic form factors

From the above observations, it will be apparent that the rainbow-ladder results for the $\{ud\}$ axial-vector diquark elastic form factors may be obtained directly from those of the ρ meson through the substitutions

$$F^{\rm em}_{1^+_{\{ud\}},j}(Q^2) = \tfrac{1}{3}F_j(Q^2)\big|^{E_\rho\to\sqrt{\frac{2}{3}}E_{qq_{1^+}}}_{m_\rho\to m_{qq_{1^+}}}. \tag{73}$$

The momentum dependence of the form factors for the $\{uu\}$ and $\{dd\}$ correlations is identical, but in these cases, the normalizations are, respectively, $\frac{4}{3}$ and $-\frac{2}{3}$.

We depict the axial-vector diquark form factors in Fig. 6. They are similar to, but distinguishable from, those of the ρ meson, falling off a little less rapidly owing to the larger mass of the axial-vector diquark. Interpolations valid on $Q^2 \in [-m^2_\rho, 10\ \text{GeV}^2]$ are

$$G^{1^+}_E(Q^2) \overset{\text{interpolation}}{=} \frac{1 - 0.16\,Q^2}{1 + 1.17\,Q^2 + 0.012\,Q^4}, \tag{74}$$

$$G^{1^+}_M(Q^2) \overset{\text{interpolation}}{=} \frac{2.13 - 0.19\,Q^2}{1 + 1.07\,Q^2 - 0.10\,Q^4}, \tag{75}$$

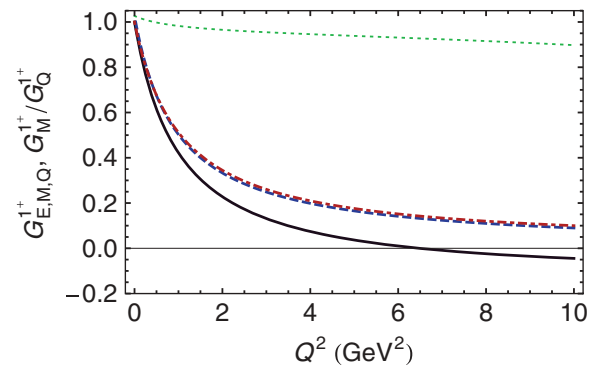

FIG. 6. (Color online) Solid curve: Pseudovector-diquark electric form factor $G^{1^+}_E(Q^2)$, which exhibits a zero at $Q^2 = 6.5$ GeV^2. (In this case, $1 - \frac{2}{3}\eta = 0$ for $Q^2 = 6m^2_{1^+} = 6.7$ GeV^2, given the computed mass of 1.06 GeV.) The dashed curve $G^{1^+}_M(Q^2)/\mu_{1^+}$ and dotted-dashed curve $G^{1^+}_Q(Q^2)/\mathcal{Q}_{1^+}$ are almost indistinguishable, as emphasized by the dotted curve $[G^{1^+}_M(Q^2)/\mu_\rho]/[G^{1^+}_Q(Q^2)/\mathcal{Q}_{1^+}]$. The charge radii and magnetic and quadrupole moments are given in Table II. Note that all form factors exhibit a pole at $Q^2 = -m^2_\rho$ because the quark-photon vertex is dressed as described in Sec. II C.

$$G_Q^{1^+}(Q^2) \stackrel{\text{interpolation}}{=} -\frac{0.81 - 0.029\,Q^2}{1 + 1.11\,Q^2 - 0.054\,Q^4}, \quad (76)$$

from which the particular pseudovector diquark form factors are obtained after multiplication by the appropriate charge factors listed in Table II.

C. 1^+- 0^+ diquark transition form factor

Owing to the flavor structure of the scalar diquark, this transition can only involve the $\{ud\}$ axial-vector diquark. It is described by a single form factor, which can be introduced through

$$T_{\mu\nu}^{0^+\gamma 1^+}(k_1, k_2) = \frac{1}{3}\frac{g_{0^+\gamma 1^+}}{m_{qq_{1^+}}}\,\epsilon_{\mu\nu\alpha\beta}k_{1\alpha}k_{2\beta}\,G^{0^+\gamma 1^+}(Q^2), \quad (77)$$

and one may readily determine that, in rainbow-ladder truncation,

$$G^{0^+\gamma 1^+}(Q^2) = G^{\pi\gamma\rho}(Q^2)\Big|_{m_\pi \to m_{qq_{0^+}}, m_\rho \to m_{qq_{1^+}}}^{(E_\pi, F_\pi, E_\rho) \to \sqrt{\frac{2}{3}}(E_{qq_{0^+}}, F_{qq_{0^+}}, E_{qq_{1^+}})}. \quad (78)$$

Computation of the form factor is straightforward and the result is depicted in Fig. 7. An interpolation valid on $Q^2 \in [-m_\rho^2, 10\ \text{GeV}^2]$ is

$$G^{0^+\gamma 1^+}(Q^2) \stackrel{\text{interpolation}}{=} \frac{1 + 0.10\,Q^2}{1 + 1.073\,Q^2}. \quad (79)$$

The associated transition radius is

$$r_{0^+\gamma 1^+} = 0.48\ \text{fm}, \quad (80)$$

which is 5% larger than $r_{\pi\gamma\rho}$ in Eq. (68), and

$$\lim_{Q^2\to\infty} G^{0^+\gamma 1^+}(Q^2) = 0.049, \quad (81)$$

just under one-half of the value in Eq. (69).

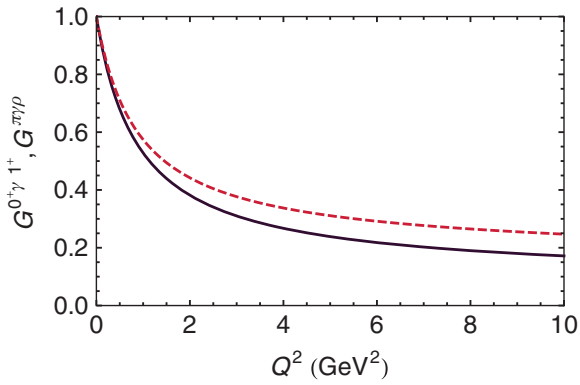

FIG. 7. (Color online) Solid curve: Momentum dependence of full result for axial-vector–scalar-diquark transition form factor $G^{0^+\gamma 1^+}(Q^2)$. Dashed curve: Result for $G^{\pi\gamma\rho}(Q^2)$ in Fig. 4. The different rates of evolution are typical of meson and diquark form factors computed herein. Note that $e_{\{ud\}}g_{0^+\gamma 1^+} = e_{\{ud\}}0.78 = 0.26$.

V. EPILOGUE

We described a unified Dyson-Schwinger equation treatment of static and electromagnetic properties of pseudoscalar- and vector-mesons and scalar- and axial-vector-diquark correlations based upon a vector-vector contact interaction. Isospin symmetry was assumed, with $m_u = m_d = m = 7$ MeV producing a physical pion mass; two parameters were used to define the gap-and Bethe-Salpeter. In a comparison with relevant static quantities, we recorded a value of 13% for the overall root-mean-square relative error.

A basic motivation for our paper is the need to document a comparison between the electromagnetic form factors of mesons and those diquarks that play a material role in nucleon structure because this is an important step toward a unified description of meson and baryon form factors based on a single interaction. A notable feature of our results, therefore, is the large degree of similarity between related form factors. For example, we find that it would be a good practical approximation to assume equality of related radii: $r_{0^+} \approx r_\pi$ and $r_{1^+} \approx r_\rho$.

As has previously been observed, a fully consistent treatment of the contact interaction produces a pion electromagnetic form factor that approaches a nonzero constant value at large spacelike momenta. On the other hand, owing to a peculiarity of the rainbow-ladder truncation, which prevents the appearance at this order of a tensor component for the ρ meson produced by a contact interaction, the ρ-meson form factors approach zero at large spacelike momenta. This accident means that a comparison with QCD-based DSE calculations can meaningfully be interpreted. In a comparison with the most sophisticated such study, the form factors produced by the contact interaction are harder, although the ratio r_π/r_ρ^E is similar. Moreover, the contact interaction's simplicity allows one to readily compute the ρ-meson form factors at arbitrarily large spacelike Q^2 and expose a zero in the electric form factor at $z_Q^2 \approx 6m_\rho^2$. Notably, $r_D z_Q^D \approx r_\rho^E z_Q^\rho$, where r_D and z_Q^D are, respectively, the deuteron's radius and the location of the zero in its electric form factor. The ρ meson's magnetic and quadrupole form factors are positive and negative definite, respectively. We reiterate that the behavior of all pseudovector-diquark form factors is semiquantitatively the same.

At the core of our analysis is a global-symmetry-preserving treatment of a vector-vector contact interaction. This has now been used in the completely consistent computation of the hadron spectrum and meson and diquark form factors. The foundation has thus been laid for the computation of baryon elastic and transition form factors, which will provide information that is crucial for the use of experimental data on such observables as a tool for charting the nature of the quark-quark interaction at long range [48].

ACKNOWLEDGMENTS

We acknowledge valuable discussions with L. Chang, I. C. Cloët, C. Hanhart, J. Rodriguez-Quintero, and S. M. Schmidt. This work was supported by the US Department of Energy, Office of Nuclear Physics, Contract No. DE-AC02-06CH11357; Forschungszentrum Jülich GmbH; the Department of Energy's Science Undergraduate Laboratory Internship program; CIC

and CONACyT grants, under Projects No. 4.10 and No. 46614-I; and the Project of Knowledge Innovation Program of the Chinese Academy of Sciences, Grant No. KJCX2.YW.W10.

APPENDIX: FORM-FACTOR FORMULAE

This Appendix is a repository for the formulae we have used to compute the form factors.

1. Elastic pion form factor

$$F_\pi^{\rm em}(Q^2) = P_T(Q^2)\big[E_\pi^2 T_{\pi,EE}^{\rm em}(Q^2) + E_\pi F_\pi T_{\pi,EF}^{\rm em}(Q^2) + F_\pi^2 T_{\pi,FF}^{\rm em}(Q^2)\big], \tag{A1}$$

where $P_T(Q^2)$ is given in Eq. (27) and

$$T_{\pi,EE}^{\rm em} = \frac{3}{4\pi^2}\left[\int_0^1 d\alpha\, \overline{\mathcal{C}}_1^{\rm iu}(\omega(M^2,\alpha,Q^2)) + 2m_\pi^2 \int_0^1 d\alpha\, d\beta\, \alpha\, \overline{\mathcal{C}}_2^{\rm iu}\big(\omega_2\big(M^2,\alpha,\beta,Q^2,m_\pi^2\big)\big)\right], \tag{A2}$$

$$T_{\pi,EF}^{\rm em} = \frac{3}{2\pi^2}\left[-\int_0^1 d\alpha\, \overline{\mathcal{C}}_1^{\rm iu}(\omega(M^2,\alpha,Q^2)) + \int_0^1 d\alpha\, d\beta\, \alpha \times \big(\alpha Q^2 - 2m_\pi^2\big)\, \overline{\mathcal{C}}_2^{\rm iu}\big(\omega_2\big(M^2,\alpha,\beta,Q^2,m_\pi^2\big)\big)\right], \tag{A3}$$

$$T_{\pi,FF}^{\rm em} = -\frac{3}{2\pi^2}\frac{1}{M^2}\int_0^1 d\alpha\, d\beta\, \alpha\big\{\mathcal{A}\big(\alpha,Q^2,m_\pi^2\big)\overline{\mathcal{C}}_1^{\rm iu}\big(\omega_2\big(M^2,\alpha,\beta,Q^2,m_\pi^2\big)\big) \tag{A4}$$

$$+\big[\mathcal{B}\big(M^2,\alpha,\beta,Q^2,m_\pi^2\big) - \mathcal{A}\big(\alpha,Q^2,m_\pi^2\big)\,\omega_2\big(M^2,\alpha,\beta,Q^2,m_\pi^2\big)\big]\overline{\mathcal{C}}_2^{\rm iu}\big(\omega_2\big(M^2,\alpha,\beta,Q^2,m_\pi^2\big)\big)\big\}, \tag{A5}$$

with

$$\mathcal{B}\big(M^2,\alpha,\beta,Q^2,m_\pi^2\big) = \alpha Q^2 M^2 + M^2 m_\pi^2(\alpha-2) + \alpha m_\pi^2\big\{\alpha Q^2[1-\alpha-2\beta(1-\beta)] + 3\alpha\beta(1-\beta)] - (1-\alpha)^2 m_\pi^2\big\}, \tag{A6}$$

$$\mathcal{A}\big(\alpha,Q^2,m_\pi^2\big) = -\tfrac{1}{2}\alpha Q^2 + \tfrac{1}{2}m_\pi^2(2-3\alpha), \tag{A7}$$

$$\omega_2\big(M^2,\alpha,\beta,Q^2,m_\pi^2\big) = M^2 + Q^2\alpha^2\beta(1-\beta) - \alpha(1-\alpha)m_\pi^2, \tag{A8}$$

where $\mathcal{C}^{\rm iu}(z)$ is defined after Eq. (9); $\mathcal{C}_1^{\rm iu}(z)$ and $\omega(M^2,\alpha,Q^2)$ in Eqs.(21) and (22); $\overline{\mathcal{C}}_1^{\rm iu}(z)$ after Eq. (27); and

$$\mathcal{C}_2^{\rm iu}(z) = \frac{1}{2}z^2\mathcal{C}''(z) = \frac{z}{2}\big(e^{-zr_{\rm uv}^2} - e^{-zr_{\rm ir}^2}\big) \tag{A9}$$

with $\overline{\mathcal{C}}_2^{\rm iu} = \mathcal{C}_2^{\rm iu}(z)/z^2$.

2. Elastic ρ-meson form factors

In generalized impulse approximation, the ρ-γ vertex in Eq. (46) becomes

$$\Lambda_{\lambda,\mu\nu} = 2N_c {\rm tr}_D \int \frac{d^4q}{(2\pi^4)} E_\rho(-p^f)\gamma_\nu^{\rm T}\, S(q+p^f)\, P_T(Q^2) i\gamma_\lambda \times S(q+p^i) E_\rho(p^i)\gamma_\mu^{\rm T}\, S(q), \tag{A10}$$

where E_ρ is the canonically normalized ρ-meson Bethe-Salpeter amplitude. Explicit expressions for the scalar functions $F_{1,2,3}(Q^2)$ can be obtained via contraction with any three sensibly chosen projection operators; the subsequent use of Feynman parametrizations yields

$$F_i(Q^2) = \frac{3}{4\pi^2}E_\rho^2 P_T(Q^2)\int_0^1 d\alpha\, d\beta\, \alpha\big[\mathcal{A}_i\,\overline{\mathcal{C}}_1^{\rm iu}(\omega_2) + [\mathcal{B}_i - \mathcal{A}_i\,\omega_2]\overline{\mathcal{C}}_2^{\rm iu}(\omega_2)\big], \tag{A11}$$

where $\mathcal{F}_i = \mathcal{F}_i(M^2,\alpha,\beta,Q^2,m_\rho^2)$, $\mathcal{F}_i = \mathcal{A}_i, \mathcal{B}_i$, viz.,

$$\mathcal{A}_1 = 2-\alpha, \tag{A12}$$

$$\mathcal{A}_2 = \frac{m_\rho^2[\alpha(10\beta-7)-4] + Q^2\alpha(2\beta-1)}{2m_\rho^2}, \tag{A13}$$

$$\mathcal{A}_3 = \frac{2\alpha(1-2\beta)\big(5m_\rho^2+Q^2\big)}{4m_\rho^2+Q^2}, \tag{A14}$$

$$\mathcal{B}_1 = 2\big[M^2(2-\alpha) + m_\rho^2\alpha(1-\alpha)^2 - \alpha^2\beta(2-\alpha)(1-\beta)Q^2\big], \tag{A15}$$

$$m_\rho^2\,\mathcal{B}_2 = m_\rho^2\big[M^2(-4-7\alpha+10\alpha\beta) - m_\rho^2(-1+\alpha)\alpha(1-7\alpha-6\beta+10\alpha\beta)\big] + \alpha\big\{M^2(-1+2\beta) + m_\rho^2\alpha[-1+2\beta + \alpha(1+\beta-5\beta^2+2\beta^3)]Q^2\big\}, \tag{A16}$$

$$\big(4m_\rho^2+Q^2\big)\mathcal{B}_3 = 4\alpha\big(m_\rho^2\big\{5M^2(1-2\beta) + m_\rho^2(-1+\alpha) \times [3-6\beta+\alpha(-5-6\beta+16\beta^2)]\big\} + \big\{M^2(1-2\beta) - m_\rho^2\alpha[-1+\alpha-2\beta + 3\alpha\beta+4\beta^2-7\alpha\beta^2+2\alpha\beta^3]\big\}Q^2\big). \tag{A17}$$

3. Vector-pseudoscalar transition form factor

The interaction vertex describing the π-ρ transition

$$T^{\pi\gamma\rho}_{\mu\nu}(k_1,k_2) = \frac{g_{\pi\gamma\rho}}{m_\rho}\epsilon_{\mu\nu\alpha\beta}k_{1\alpha}k_{2\beta}G^{\pi\gamma\rho}(Q^2)$$
$$= \mathrm{tr}_D\int\frac{d^4\ell}{(2\pi)^4}\Gamma_\pi(-P)S(\ell_2)\,P_T(Q^2)\,i\gamma_\mu$$
$$\times S(\ell_{12})\,i\Gamma^\rho_\nu(k_2)\,S(\ell_1), \tag{A18}$$

where the incoming ρ meson has momentum k_2, the photon has momentum $k_1 = Q$, the outgoing pion has momentum $P = (k_1 + k_2)$, and $\ell_1 = \ell - k_1$, $\ell_2 = \ell + k_2$, $\ell_{12} = \ell - k_1 + k_2$. In this instance, the kinematic constraints are

$$k_1^2 = -Q^2, \quad k_2^2 = -m_\rho^2, \quad 2\,k_1\cdot k_2 = m_\rho^2 - m_\pi^2 - Q^2. \tag{A19}$$

Given the structure of the pion's Bethe-Salpeter amplitude, one may write

$$G^{\pi\gamma\rho}(Q^2) = G_E^{\pi\gamma\rho}(Q^2) + G_F^{\pi\gamma\rho}(Q^2), \tag{A20}$$

wherein

$$G_E^{\pi\gamma\rho}(Q^2) = \frac{E_\pi\mathcal{E}_\rho}{2\pi^2}M\,P_T(Q^2)\int_0^1 d\alpha\,d\beta\,\alpha\,\bar{\mathcal{C}}_2^{\mathrm{ir}}(\omega_3), \tag{A21}$$

$$\hat{G}_F^{\pi\gamma\rho}(Q^2) = -\frac{F_\pi\mathcal{E}_\rho}{4\pi^2}\frac{1}{M}P_T(Q^2)\int_0^1 d\alpha\,d\beta\,\alpha\left[f_1^{\pi\gamma\rho}\bar{\mathcal{C}}_1^{\mathrm{ir}}(\omega_3)\right.$$
$$\left.+\left(f_0^{\pi\gamma\rho} - \omega_3\,f_1^{\pi\gamma\rho}\right)\bar{\mathcal{C}}_2^{\mathrm{ir}}(\omega_3)\right], \tag{A22}$$

with

$$\omega_3 := \omega_3\left(M^2,\alpha,\beta,m_\rho^2,m_\pi^2,Q^2\right) = M^2 - \alpha\big[\alpha\beta(1-\beta)m_\pi^2$$
$$+(1-\alpha)(1-\beta)m_\rho^2 - (1-\alpha)\beta\,Q^2\big] \tag{A23}$$

and

$$f_1^{\pi\gamma\rho} = 2 - 3\alpha, \tag{A24}$$
$$f_0^{\pi\gamma\rho} = (2-\alpha)\big[M^2 + \alpha^2\beta(1-\beta)m_\pi^2\big]$$
$$+(1-\alpha)^2\big[\alpha(1-\beta)m_\rho^2 - \alpha\beta\,Q^2\big]. \tag{A25}$$

The vertex in Eq. (A18) is intimately connected with the Abelian anomaly, which describes the process $\pi^0 \to \gamma\gamma$ and associated transition form factors. The manner by which all aspects of the anomaly may be reproduced in the model we are considering is detailed in Secs. III A and III B 2 of Ref. [46]. In the present context, consistency with the anomaly requires that, in Eqs. (A21) and (A22), $\mathcal{E}_\rho = E_\rho/\mathcal{N}_{\pi\gamma\gamma}$, with $\mathcal{N}_{\pi\gamma\gamma}$ defined such that $G^{\pi\gamma\gamma}(Q^2=0) = 1/2$ and $G_F^{\pi\gamma\rho}(Q^2) = \hat{G}_F^{\pi\gamma\rho}(Q^2) - \hat{G}_F^{\pi\gamma\rho}(0)$. Both modifications are necessary in order to correct for the dynamical role played by the ultraviolet cutoff in a contact-interaction theory.

[1] C. D. Roberts and A. G. Williams, Prog. Part. Nucl. Phys. **33**, 477 (1994).
[2] C. D. Roberts and S. M. Schmidt, Prog. Part. Nucl. Phys. **45**, S1 (2000).
[3] A. Bashir, A. Raya, I. C. Cloët, and C. D. Roberts, Phys. Rev. C **78**, 055201 (2008).
[4] A. Kizilersu and M. R. Pennington, Phys. Rev. D **79**, 125020 (2009).
[5] A. Bashir, A. Raya, S. Sanchez-Madrigal, and C. D. Roberts, Few-Body Syst. **46**, 229 (2009).
[6] L. Chang, Y. X. Liu, and C. D. Roberts, Phys. Rev. Lett. **106**, 072001 (2011).
[7] J. Praschifka, C. D. Roberts, and R. T. Cahill, Phys. Rev. D **36**, 209 (1987).
[8] C. D. Roberts, R. T. Cahill, and J. Praschifka, Ann. Phys. (NY) **188**, 20 (1988).
[9] R. T. Cahill, C. D. Roberts, and J. Praschifka, Phys. Rev. D **36**, 2804 (1987).
[10] J. Praschifka, R. T. Cahill, and C. D. Roberts, Int. J. Mod. Phys. A **4**, 4929 (1989).
[11] H. J. Munczek and P. Jain, Phys. Rev. D **46**, 438 (1992).
[12] L. C. L. Hollenberg, C. D. Roberts, and B. H. J. McKellar, Phys. Rev. C **46**, 2057 (1992).
[13] P. Jain and H. J. Munczek, Phys. Rev. D **48**, 5403 (1993).
[14] K. L. Mitchell, P. C. Tandy, C. D. Roberts, and R. T. Cahill, Phys. Lett. B **335**, 282 (1994).
[15] H. J. Munczek, Phys. Rev. D **52**, 4736 (1995).
[16] M. R. Frank and C. D. Roberts, Phys. Rev. C **53**, 390 (1996).
[17] A. Bender, C. D. Roberts, and L. Von Smekal, Phys. Lett. B **380**, 7 (1996).
[18] C. J. Burden, L. Qian, C. D. Roberts, P. C. Tandy, and M. J. Thomson, Phys. Rev. C **55**, 2649 (1997).
[19] P. Maris, C. D. Roberts, and P. C. Tandy, Phys. Lett. B **420**, 267 (1998).
[20] P. Maris and C. D. Roberts, Phys. Rev. C **56**, 3369 (1997).
[21] M. A. Pichowsky, S. Walawalkar, and S. Capstick, Phys. Rev. D **60**, 054030 (1999).
[22] P. Maris and P. C. Tandy, Phys. Rev. C **60**, 055214 (1999).
[23] P. Maris, Few-Body Syst. **32**, 41 (2002).
[24] A. Höll, A. Krassnigg, and C. D. Roberts, Phys. Rev. C **70**, 042203 (2004).
[25] M. S. Bhagwat, L. Chang, Y. X. Liu, C. D. Roberts, and P. C. Tandy, Phys. Rev. C **76**, 045203 (2007).
[26] L. Chang and C. D. Roberts, Phys. Rev. Lett. **103**, 081601 (2009).
[27] C. S. Fischer and R. Williams, Phys. Rev. Lett. **103**, 122001 (2009).
[28] C. D. Roberts, R. T. Cahill, M. E. Sevior, and N. Iannella, Phys. Rev. D **49**, 125 (1994).
[29] C. D. Roberts, Nucl. Phys. A **605**, 475 (1996).
[30] R. Alkofer and C. D. Roberts, Phys. Lett. B **369**, 101 (1996).
[31] P. Maris and C. D. Roberts, Phys. Rev. C **58**, 3659 (1998).
[32] D. Kekez and D. Klabučar, Phys. Lett. B **457**, 359 (1999).
[33] P. Maris and P. C. Tandy, Phys. Rev. C **61**, 045202 (2000).
[34] B. Bistrović and D. Klabučar, Phys. Lett. B **478**, 127 (2000).
[35] P. Maris and P. C. Tandy, Phys. Rev. C **62**, 055204 (2000).
[36] M. B. Hecht, C. D. Roberts, and S. M. Schmidt, Phys. Rev. C **63**, 025213 (2001).
[37] P. Bicudo, S. Cotanch, F. Llanes-Estrada, P. Maris, E. Ribeiro, and A. Szczepaniak, Phys. Rev. D **65**, 076008 (2002).
[38] P. Maris and P. C. Tandy, Phys. Rev. C **65**, 045211 (2002).
[39] D. Jarecke, P. Maris, and P. C. Tandy, Phys. Rev. C **67**, 035202 (2003).
[40] S. R. Cotanch and P. Maris, Phys. Rev. D **68**, 036006 (2003).

[41] P. Maris, Few-Body Syst. **35**, 117 (2004).
[42] A. Höll, A. Krassnigg, P. Maris, C. D. Roberts, and S. V. Wright, Phys. Rev. C **71**, 065204 (2005).
[43] M. S. Bhagwat and P. Maris, Phys. Rev. C **77**, 025203 (2008).
[44] L. X. Gutiérrez-Guerrero, A. Bashir, I. C. Cloët, and C. D. Roberts, Phys. Rev. C **81**, 065202 (2010).
[45] R. J. Holt and C. D. Roberts, Rev. Mod. Phys. **82**, 2991 (2010).
[46] H. L. L. Roberts, C. D. Roberts, A. Bashir, L. X. Gutierrez-Guerrero, and P. C. Tandy, Phys. Rev. C **82**, 065202 (2010).
[47] T. Nguyen, A. Bashir, C. D. Roberts, and P. C. Tandy, Phys. Rev. C (in press), arXiv:1102.2448.
[48] I. Aznauryan *et al.*, arXiv:0907.1901.
[49] R. T. Cahill, C. D. Roberts, and J. Praschifka, Aust. J. Phys. **42**, 129 (1989).
[50] H. L. L. Roberts, L. Chang, I. C. Cloët, and C. D. Roberts,, Few-Body Syst. **51**, 1 (2011).
[51] H. L. L. Roberts, L. Chang, I. C. Cloët, and C. D. Roberts, in *Proceedings of the Workshop: Exclusive Reactions at High Momentum Transfer IV*, edited by A. Radyushkin (World Scientific, New Jersey, 2011), pp. 201–211.
[52] G. Eichmann, R. Alkofer, I. C. Cloet, A. Krassnigg, and C. D. Roberts, Phys. Rev. C **77**, 042202 (2008).
[53] G. Eichmann, I. C. Cloet, R. Alkofer, A. Krassnigg, and C. D. Roberts, Phys. Rev. C **79**, 012202 (2009).
[54] I. C. Cloët *et al.*, Few-Body Syst. **46**, 1 (2009).
[55] K. de Jager, Int. J. Mod. Phys. E **19**, 844 (2010).
[56] A. J. R. Puckett *et al.*, Phys. Rev. Lett. **104**, 242301 (2010).
[57] S. Riordan *et al.*, Phys. Rev. Lett. **105**, 262302 (2010).
[58] W. Kamleh, P. O. Bowman, D. B. Leinweber, A. G. Williams, and J. Zhang, Phys. Rev. D **76**, 094501 (2007).
[59] D. Dudal, J. A. Gracey, S. P. Sorella, N. Vandersickel, and H. Verschelde, Phys. Rev. D **78**, 125012 (2008).
[60] A. Cucchieri and T. Mendes, Phys. Rev. D **81**, 016005 (2010).
[61] J. Rodriguez-Quintero, J. High Energy Phys. 01 (**2011**) 105.
[62] J. I. Skullerud *et al.*, J. High Energy Phys. 04 (**2003**) 047.
[63] L. Chang and C. D. Roberts, arXiv:1003.5006.
[64] Y. Nambu and G. Jona-Lasinio, Phys. Rev. **122**, 345 (1961); **124**, 246 (1961).
[65] H. J. Munczek and A. M. Nemirovsky, Phys. Rev. D **28**, 181 (1983).
[66] D. Ebert, T. Feldmann, and H. Reinhardt, Phys. Lett. B **388**, 154 (1996).
[67] G. Krein, C. D. Roberts, and A. G. Williams, Int. J. Mod. Phys. A **7**, 5607 (1992).
[68] C. D. Roberts, Prog. Part. Nucl. Phys. **61**, 50 (2008).
[69] C. H. Llewellyn-Smith, Ann. Phys. (NY) **53**, 521 (1969).
[70] H. L. L. Roberts, L. Chang, and C. D. Roberts, Int. J. Mod. Phys. A **26**, 371 (2011).
[71] C. J. Burden, J. Praschifka, and C. D. Roberts, Phys. Rev. D **46**, 2695 (1992).
[72] S. J. Brodsky, C. D. Roberts, R. Shrock, and P. C. Tandy, Phys. Rev. C **82**, 022201(R) (2010).
[73] I. C. Cloet, W. Bentz, and A. W. Thomas, Phys. Rev. Lett. **95**, 052302 (2005).
[74] J. Bijnens, Prog. Part. Nucl. Phys. **58**, 521 (2007).
[75] P. Maris and P. C. Tandy, Nucl. Phys. B, Proc. Suppl. **161**, 136 (2006).
[76] A. C. Aguilar, D. Binosi, J. Papavassiliou, and J. Rodriguez-Quintero, Phys. Rev. D **80**, 085018 (2009).
[77] A. C. Aguilar, D. Binosi, and J. Papavassiliou, J. High Energy Phys. 07 (**2010**) 002.
[78] S. J. Brodsky and G. F. de Teramond, Acta Phys. Pol. B **41**, 2605 (2010).
[79] K. Nakamura *et al.*, J. Phys. G: Nucl. Part. Phys. **37**, 075021 (2010).
[80] R. Alkofer, A. Bender, and C. D. Roberts, Int. J. Mod. Phys. A **10**, 3319 (1995).
[81] S. J. Brodsky and J. R. Hiller, Phys. Rev. D **46**, 2141 (1992).
[82] C. J. Burden, C. D. Roberts, and M. J. Thomson, Phys. Lett. B **371**, 163 (1996).
[83] F. T. Hawes and M. A. Pichowsky, Phys. Rev. C **59**, 1743 (1999).
[84] J. P. B. C. de Melo, H. W. L. Naus, and T. Frederico, Phys. Rev. C **59**, 2278 (1999).
[85] J. P. B. C. de Melo and T. Frederico, Phys. Rev. C **55**, 2043 (1997).
[86] H. M. Choi and C. R. Ji, Phys. Rev. D **59**, 074015 (1999).
[87] H. M. Choi and C. R. Ji, Phys. Rev. D **70**, 053015 (2004).
[88] M. Kohl, Nucl. Phys. A **805**, 361 (2008).
[89] M. I. Krivoruchenko, Sov. J. Nucl. Phys. **45**, 503 (1987) [Yad. Fiz. **45**, 809 (1987)]; Z. Phys. C: Part. Fields **36**, 243 (1987).
[90] J. N. Hedditch, W. Kamleh, B. G. Lasscock, D. B. Leinweber, A. G. Williams, and J. M. Zanotti, Phys. Rev. D **75**, 094504 (2007).
[91] C. Alexandrou and G. Koutsou, Phys. Rev. D **78**, 094506 (2008).
[92] J. C. R. Bloch, C. D. Roberts, S. M. Schmidt, A. Bender, and M. R. Frank, Phys. Rev. C **60**, 062201 (1999).